NASA TN D-1923

TECHNICAL NOTE

D-1923

STUDY OF A GUIDANCE SCHEME USING APPROXIMATE SOLUTIONS OF TRAJECTORY EQUATIONS TO CONTROL THE AERODYNAMIC SKIP FLIGHT OF A REENTRY VEHICLE

By Robert S. Dunning

Langley Research Center
Langley Station, Hampton, Va.

NATIONAL AERONAUTICS AND SPACE ADMINISTRATION

WASHINGTON August 1963

NATIONAL AERONAUTICS AND SPACE ADMINISTRATION

TECHNICAL NOTE D-1923

STUDY OF A GUIDANCE SCHEME USING APPROXIMATE SOLUTIONS OF TRAJECTORY EQUATIONS TO CONTROL THE AERODYNAMIC SKIP FLIGHT OF A REENTRY VEHICLE

By Robert S. Dunning

SUMMARY

Approximate closed-form solutions to the reentry equations are developed by assuming that the difference between the centrifugal and gravitational accelerations is negligible. The approximate solutions are valid in the exit-velocity range between approximately 23,000 and 26,000 feet per second. A numerical comparison is made between the approximate and exact solutions for six typical trajectories. The results indicate good agreement with complete convergence occurring at the skipout condition within a reasonable flight corridor. Approximate explicit equations governing coasting flight after a skip maneuver are also developed and compared with the exact solutions. A guidance scheme employing these equations is described and results are presented from a two-dimensional digital-computer simulation of this scheme. Emphasis is placed on simplicity and speed of computation. The results indicate satisfactory control to exit from the atmosphere over ranges from approximately 70° to 200° about the center of the earth.

INTRODUCTION

Although direct reentry into the atmosphere is planned for vehicles returning from space missions, a "skip" type of reentry may be useful as a means of extending range or as an emergency procedure if suitable guidance can be provided. In a skip maneuver the vehicle enters the atmosphere at a low flight-path angle and then, through the control of aerodynamic and centrifugal forces, is made to skip out. After a period of coasting flight, the vehicle reenters. Such a maneuver has the advantages that the heat input to the vehicle may be reduced in relation to the range covered and that such a maneuver may be more compatible to the heat-protection system of the vehicle.

The total angular range covered is composed of three portions: a portion within the atmosphere from reentry to exit, a coasting portion outside of the atmosphere, and a portion from final reentry to landing. Of the three parts, the first and third will in most cases contribute less to the total range than the coast portion; but the conditions that exist at the exit from the first part essentially determine the range that one may reach. The first problem in the use

of a skip maneuver is, then, to select the total range required and to establish exit conditions from the atmosphere which will insure that this range is achieved. That is, from among the numerous possible velocity—flight-path-angle combinations one must select a single combination which will achieve the desired range. At the same time, this combination must be such that it is not only physically possible for the vehicle to be guided to it during the atmospheric portion of the maneuver, but this combination must also allow for the limitation that the speed cannot be materially controlled by aerodynamic drag once the initial reentry has been initiated. Moreover, once a proper combination of exit velocity and flight-path angle has been selected, it is necessary to guide the vehicle to achieve these conditions very accurately, inasmuch as relatively small errors at exit can have a pronounced effect on range.

In addition to the foregoing requirements, it is also desirable that any practical skip-control guidance system be simple and be capable of controlling the vehicle rapidly and accurately in response to present-time information about velocity and flight-path angle.

In this report some preliminary results are presented of an analytic study which has been made with a view of providing just such control. It must be emphasized that this is a fine-adjustment scheme to be utilized within an already reasonable flight corridor. The guidance equations for the first atmospheric portion are developed, then the coasting portion is considered in order to determine desirable exit conditions; and, finally, some preliminary results of a simulation combining the two portions are discussed. No attempt is made to cover the second entry portion of the maneuver because this is a normal reentry and hence is already adequately covered in other literature. (See refs. 1 and 2.) For the sake of simplicity, the whole study has been kept two dimensional.

CONSTANTS AND SYMBOLS

Coordinates employed in describing the motions of the reentry vehicle are given in figure 1. Any consistent set of units may be used. In this report it is assumed that:

g_e = 32.17 feet per second per second

r_e = 3,960 international statute miles

V_{cir} = 25,750 feet per second

β = 1/24,000 per foot

ρ_e = 0.003 slug per cubic foot

1 international statute mile = 5,280 feet = 1.609344 kilometers

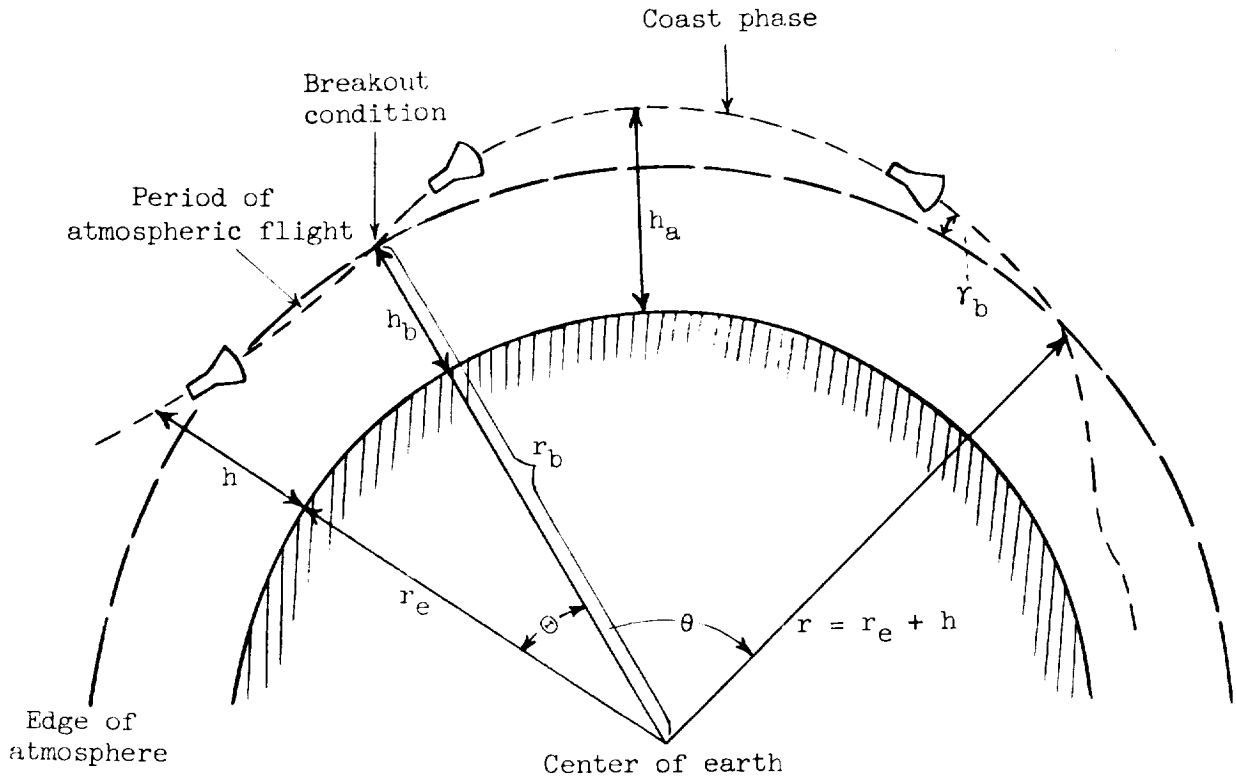

Figure 1.- Coordinates employed in describing motions of reentry vehicle.

A,B,C	constants defined by equations (23), (24), and (25)
A',B',C'	constants defined by equations (40), (41), and (42)
a	constant defined as $\cos \gamma_b - \frac{K_2}{\beta} y_b$
b	constant defined as $\frac{K_2}{\beta}$
C_D	drag coefficient
C_L	lift coefficient
D	drag force
g	gravitational acceleration
g_e	earth gravitational constant
h	radial height above surface of earth
h_a	maximum (apogee) altitude attained by vehicle
h_p	minimum (perigee) altitude attained by vehicle
K_1	constant defined as $\frac{C_D \rho_e S}{2m}$
K_2	constant defined as $\frac{C_L \rho_e S}{2m}$
L	lift force
L/D	lift-drag ratio
m	mass of vehicle
q	dynamic pressure
r	radial distance of entry vehicle from center of earth, $r_e + h$
r_e	radius of earth
r_b	exit, or breakout, distance from center of earth
s	distance traveled

S	surface area of entry vehicle
t	time
V	velocity
V_{cir}	circular satellite velocity
V_b	exit, or breakout, velocity
W	weight of entry vehicle
$\dot{x}$	horizontal velocity component at exit, or breakout, $V_b \cos \gamma_b$
$\bar{Y}$	function of a, b, and y defined by equation (15)
y	function of altitude, $e^{-\beta h}$
z	function of y defined in equation (15b)
$\dot{z}$	vertical velocity component at exit, $V_b \sin \gamma_b$
α	angle of attack
β	decay constant of atmosphere
Γ	function defined by equations (20)
γ	flight-path angle
γ_b	exit, or breakout, flight-path angle
$\epsilon(V)$	function of velocity, $\frac{g}{V^2}\left(\frac{V^2}{gr} - 1\right)\cos \gamma$
Θ	range measured in angle about center of earth during skip portion of maneuver
θ	range measured in angle about center of earth during coast portion of maneuver
ρ	density of atmosphere

Subscripts:

a	apogee or highest trajectory point
b	breakout, or exit, conditions

c	approximate solutions
e	conditions existing at surface of earth
max	maximum

Bars over symbols denote special conditions indicated in text.

Dots over symbols denote derivatives with respect to time.

ATMOSPHERIC REENTRY PORTION

In order to provide the requisite degree of accuracy and, at the same time, to maintain as simple an operational procedure as possible, the equations of motion will be solved in a simple two-dimensional form. This approach is attractive both from the computational standpoint because solutions based on present conditions must be provided quickly, and from the operational standpoint because the equations can then be incorporated into a small memory unit attached to a general-purpose computer and need not be read into the computer at all unless actually needed.

Inasmuch as the coast phase will be entirely determined by the velocity and flight-path angle which exist when the vehicle exits from the atmosphere, the primary purpose in solving these equations is to provide a means of guiding the vehicle to a certain previously supplied exit velocity and flight-path angle. A method of supplying exit velocity and flight-path angle will be considered later in this report as a part of the coasting phase. However, as far as the atmospheric reentry portion is concerned (i.e., that portion which constitutes the first part of this report) the breakout or exit conditions will be taken as externally supplied.

Equations and Assumptions

The basic nonlinear equations of motion for atmospheric reentry are:

$$\left.\begin{aligned} m\dot{V} &= -D - W \sin \gamma \\ mV\dot{\gamma} &= L + W\left(\frac{V^2}{gr} - 1\right)\cos \gamma \\ \dot{h} &= V \sin \gamma \\ r\dot{\theta} &= V \cos \gamma \end{aligned}\right\} \qquad (1)$$

For simplification of these equations, the following substitutions and assumptions are made:

$$\rho = \rho_e e^{-\beta h}$$

where ρ_e and β are constants;

$$\frac{D}{m} = K_1 e^{-\beta h} V^2$$

where $K_1 = \frac{C_D \rho_e S}{2m} = \text{Constant}$;

$$\frac{L}{m} = K_2 e^{-\beta h} V^2$$

where $K_2 = \frac{C_L \rho_e S}{2m} = \text{Constant}$; and

$$\frac{g}{V^2}\left(\frac{V^2}{gr} - 1\right)\cos \gamma = \epsilon(V) \approx 0$$

From the last assumption it is seen that whenever the velocity is equal to satellite velocity, that is, $V = \sqrt{gr}$, or when $\gamma = 90^\circ$, the term $\epsilon(V)$ is identically zero. Hence, these closed-form solutions to the reentry equations are developed by assuming that the difference between the centrifugal and gravitational accelerations is negligible. The term $\epsilon(V)$ will be carried, however, until this assumption can be justified.

For simplicity, the following change of the variable h to the variable y is made. Let

$$y = e^{-\beta h} \tag{2}$$

so that

$$\frac{\dot{y}}{y} = -\beta \dot{h} \tag{2a}$$

With the foregoing assumptions and the change of variables given by equations (2) and (2a), the equations of motion (1) become:

$$\left.\begin{aligned} \dot{V} &= -K_1 y V^2 - g \sin \gamma \\ \dot{\gamma} &= K_2 y V + V\epsilon(V) \\ \dot{y} &= -\beta y V \sin \gamma \\ r\dot{\theta} &= V \cos \gamma \end{aligned}\right\} \tag{3}$$

Eliminate the independent variable, time, in favor of the variable y. Equations (3) then become:

$$\frac{dV}{dy} = \frac{\dot{V}}{\dot{y}} = \frac{K_1 V}{\beta \sin \gamma} + \frac{g}{\beta y V} \tag{4}$$

$$\frac{d\gamma}{dy} = \frac{\dot{\gamma}}{\dot{y}} = -\frac{K_2}{\beta \sin \gamma} - \frac{\epsilon(V)}{\beta y \sin \gamma} \tag{5}$$

and

$$\frac{d\Theta}{dy} = \frac{\dot{\Theta}}{\dot{y}} = -\frac{\operatorname{ctn} \gamma}{\beta r y} \tag{6}$$

These, then, are the equations to be integrated for V, γ, and Θ as functions of the variable y, which in turn is expressible in terms of the altitude h. It should be noted that no assumption has been made as to the magnitude of γ; that is, no assumption of a small flight-path angle has been made.

Variation of Flight-Path Angle γ

In order that the flight-path angle γ be evaluated, the following steps are taken. With the use of the subscript b to denote the exit or breakout condition, the integral of equation (5) becomes:

$$\int_{\gamma}^{\gamma_b} \sin \gamma \, d\gamma = -\frac{K_2}{\beta} \int_{y}^{y_b} dy - \frac{1}{\beta} \int_{y}^{y_b} \frac{\epsilon(V) dy}{y}$$

If, during the interval of evaluation, $\epsilon(V)$ has a very weak variation with y, then

$$-\cos \gamma \Big|_{\gamma}^{\gamma_b} = -\frac{K_2}{\beta} y \Big|_{y}^{y_b} - \frac{\epsilon(V)}{\beta} \ln y \Big|_{y}^{y_b}$$

or

$$\cos \gamma = \cos \gamma_b + \frac{K_2}{\beta}(y - y_b) + \frac{\epsilon(V)}{\beta} \ln \frac{y}{y_b} \tag{7}$$

In terms of h, equation (7) becomes:

$$\cos \gamma = \cos \gamma_b + \frac{K_2}{\beta}\left(e^{-\beta h} - e^{-\beta h_b}\right) - \epsilon(V)\left(h - h_b\right) \tag{8}$$

Since, for the appropriate values of βh and βh_b

$$\frac{1}{\beta}\left(e^{-\beta h} - e^{-\beta h_b}\right) \approx -\left(h - h_b\right)$$

and $K_2 \gg \epsilon(V)$, it can be seen that the third term on the right-hand side of equation (8) is negligible compared to the second term on the right-hand side and is henceforth neglected.

Variation of the Velocity V

For the purpose of evaluating velocity V as a function of y, equation (7) is written in the form

$$\cos \gamma = a + by \tag{9}$$

where

$$a = \cos \gamma_b - \frac{K_2}{\beta} y_b \tag{10}$$

and

$$b = \frac{K_2}{\beta} \tag{11}$$

Equation (9) may be rewritten:

$$\sin \gamma = \sqrt{1 - (a + by)^2} \tag{12}$$

or

$$\sin \gamma = \sqrt{\left(1 - a^2\right) - 2aby - b^2y^2} \tag{12a}$$

Equation (4) then becomes

$$\frac{dV}{V} = \frac{1}{\beta}\left(\frac{K_1}{\sin \gamma} + \frac{g}{V^2 y}\right)dy$$

and the integral of this equation with the proper limits yields

$$\int_V^{V_b} \frac{dV}{V} = \frac{1}{\beta} \int_y^{y_b} \left(\frac{K_1}{\sin \gamma} + \frac{g}{V^2 y}\right)dy \tag{13}$$

Again, it may be seen from numerical calculations that the second term on the right-hand side of equation (13) will contribute very little to the solution because $\frac{K_1}{\sin \gamma} \gg \frac{g}{V^2}$ by several orders of magnitude. Furthermore, the small variations in g and V with y throughout the interval of integration will have even less influence on the solution and will therefore be neglected. Treating g and V in the second term of the right-hand side of equation (4) as constant average values (denoted by $\bar{g}$ and $\bar{V}$) and replacing $\sin \gamma$ with the identity of equation (12a) alters equation (13) to

$$\ln \frac{V}{V_b} = -\frac{K_1}{\beta} \int_y^{y_b} \frac{dy}{\sqrt{\bar{Y}}} + \frac{\bar{g}}{\beta \bar{V}^2} \ln \frac{y}{y_b} \tag{14}$$

where

$$\bar{Y} = \left(1 - a^2\right) - 2aby - b^2 y^2 \tag{15}$$

By the use of integral tables and several trigometric identities, the integral of the first term on the right-hand side of equation (14) may be put into the form

$$\int \frac{dy}{\sqrt{\bar{Y}}} = \frac{-1}{\pm b} \sin^{-1}\left(-\frac{a + by}{\pm 1}\right)$$

From equations (11) and (9),

$$\int \frac{dy}{\sqrt{\bar{Y}}} = \mp \frac{\beta}{K_2} \sin^{-1}\left(\frac{-\cos \gamma}{\pm 1}\right)$$

$$= \mp \frac{\beta}{K_2}\left[\frac{\pi}{2} - \cos^{-1}\left(\frac{-\cos \gamma}{\pm 1}\right)\right]$$

Depending on the choice of signs for the second term of the right-hand side of the preceding equation, the integral of $\frac{dy}{\sqrt{\bar{Y}}}$ may become

$$\int \frac{dy}{\sqrt{\bar{Y}}} = \pm \frac{\beta}{K_2}\left(\frac{\pi}{2} - \gamma\right) \tag{16a}$$

or

$$\int \frac{dy}{\sqrt{\bar{Y}}} = \pm \frac{\beta}{K_2}\left(\frac{\pi}{2} + \gamma\right) \tag{16b}$$

In either case, the same answer results when the limits of equation (14) are applied, and when the values of equations (16) are substituted into equation (14), namely,

$$\ln \frac{V}{V_b} = \pm \frac{K_1}{K_2}(\gamma - \gamma_b) + \frac{\bar{g}}{\beta \bar{V}^2} \ln \frac{y}{y_b}$$

Clearing logarithms and replacing y with $e^{-\beta h}$ and K_1/K_2 with $\frac{1}{(L/D)}$ yields the following explicit expression for V:

$$V = V_b e^{\left[\frac{\pm D}{L}(\gamma-\gamma_b) - \frac{\bar{g}}{\bar{V}^2}(h-h_b)\right]} \tag{17}$$

Again it should be noted that equation (17) is valid only in an interval in which the second term of the exponent is always small compared to the first term. This second term should be considered an approximate second-order correction to the first term by virtue of its derivation. It also follows that inasmuch as V_b must always be less than V (because of atmospheric drag) the first term of the exponent must always be a positive quantity. Finally, because a value of $\bar{g}/\bar{V}^2$ must be assigned in equation (14), it should suffice to use g_b and V_b if one is solving for V and to use the present-state values of g and V if one is solving for V_b.

Variation of Range Θ

Integration of equation (6) for range yields the following equations:

$$\int_{\Theta}^{\Theta_b} d\Theta = -\frac{1}{\beta r} \int_{y}^{y_b} \frac{\operatorname{ctn} \gamma \, dy}{y}$$

$$\int_{\Theta}^{\Theta_b} d\Theta = \frac{1}{\beta r} \int_{y_b}^{y} \frac{(a + by)}{\sqrt{1 - (a + by)^2}} \frac{dy}{y}$$

and

$$\int_{\Theta}^{\Theta_b} d\Theta = \frac{a}{\beta r} \int_{y_b}^{y} \frac{dy}{y\sqrt{\overline{Y}}} + \frac{b}{\beta r} \int_{y_b}^{y} \frac{dy}{\sqrt{\overline{Y}}}$$

At this point, three cases must be considered. First, if $a^2 = 1$, then

$$\Theta_b - \Theta = \frac{a}{\beta r}\left(\frac{\sqrt{\overline{Y}}}{aby}\right)_{y_b}^{y} + \frac{b}{\beta r}\left[\pm \frac{\beta}{K_2} \sin^{-1}\left(\frac{-\cos \gamma}{\pm 1}\right)\right]_{\gamma}^{\gamma_b}$$

$$\Theta_b - \Theta = \pm \frac{1}{K_2 r}\left(\frac{\sin \gamma}{y} - \frac{\sin \gamma_b}{y_b}\right) \pm \frac{1}{\beta r}(\gamma - \gamma_b)$$

$$\Theta_b - \Theta = \pm \frac{1}{K_2 r}\left(e^{\beta h} \sin \gamma - e^{\beta h_b} \sin \gamma_b\right) \pm \frac{1}{\beta r}(\gamma - \gamma_b) \qquad (18a)$$

In most practical cases a^2 is very nearly unity, therefore equation (18a) will usually suffice. However, the following possibilities are included for the sake of completeness.

Second, if $a^2 < 1$, then

$$\Theta_b - \Theta = \pm \frac{a}{\beta r\sqrt{1 - a^2}}\left[-\ln\left(\frac{\sqrt{\overline{Y}} + \sqrt{1 - a^2}}{y} - \frac{ab}{\sqrt{1 - a^2}}\right)\right]_{y_b}^{y} \pm \frac{1}{\beta r}(\gamma - \gamma_b)$$

$$\Theta_b - \Theta = \pm \frac{a}{\beta r\sqrt{1 - a^2}}\left[-\ln\left(\frac{\sin\gamma + \sqrt{1 - a^2}}{y} - \frac{ab}{\sqrt{1 - a^2}}\right)\right.$$

$$\left. + \ln\left(\frac{\sin\gamma_b + \sqrt{1 - a^2}}{y_b} - \frac{ab}{\sqrt{1 - a^2}}\right)\right] \pm \frac{1}{\beta r}(\gamma - \gamma_b)$$

$$\Theta_b - \Theta = \pm \frac{a}{\beta r\sqrt{1 - a^2}}\left[\ln\left(\frac{1 - a^2 - aby_b + \sqrt{1 - a^2}\sin\gamma_b}{1 - a^2 - aby + \sqrt{1 - a^2}\sin\gamma}\frac{y}{y_b}\right)\right] \pm \frac{1}{\beta r}(\gamma - \gamma_b)$$

$$\Theta_b - \Theta = \pm \frac{a}{\beta r\sqrt{1 - a^2}}\left[\ln\frac{z(y_b)}{z(y)} - \beta(h - h_b)\right] \pm \frac{1}{\beta r}(\gamma - \gamma_b) \qquad (18b)$$

where $z(y) = 1 - a^2 - aby + \sqrt{1 - a^2}\sin\gamma$.

And third, if $a^2 > 1$, then

$$\Theta_b - \Theta = \pm \frac{a}{\beta r}\frac{1}{\sqrt{a^2 - 1}}\left[\sin^{-1}\left(\frac{-aby + 1 - a^2}{\pm by}\right)\right]_{y_b}^{y} \pm \frac{1}{\beta r}(\gamma - \gamma_b)$$

$$\Theta_b - \Theta = \pm \frac{a}{\beta r\sqrt{a^2 - 1}}\left[\sin^{-1}\left(\frac{1 - a^2 - aby}{\pm by}\right) - \sin^{-1}\left(\frac{1 - a^2 - aby_b}{\pm by_b}\right)\right] \pm \frac{1}{\beta r}(\gamma - \gamma_b)$$

$$\Theta_b - \Theta = \pm \frac{a}{\beta r\sqrt{a^2 - 1}}\left\{\sin^{-1}\left[\frac{\beta(1 - a\cos\gamma)}{\pm K_2 y}\right] - \sin^{-1}\left[\frac{\beta(1 - a\cos\gamma_b)}{\pm K_2 y_b}\right]\right\} \pm \frac{1}{\beta r}(\gamma - \gamma_b)$$

(18c)

In a more compact form, equations (18a), (18b), and (18c) may be expressed as

$$\Theta_b - \Theta = \frac{1}{\beta r}\left[\Gamma(\gamma,h) \pm \left(\gamma - \gamma_b\right)\right] \tag{19}$$

where the negative sign on the term in brackets is the proper choice in all cases, and where, for the first case when $a^2 = 1$,

$$\Gamma(\gamma,h) = \pm \frac{\beta}{K_2}\left(e^{\beta h}\sin\gamma - e^{\beta h_b}\sin\gamma_b\right) \tag{20a}$$

for the second case when $a^2 < 1$,

$$\Gamma(\gamma,h) = \pm \frac{a}{\sqrt{1 - a^2}}\left[\beta\left(h_b - h\right) + \ln\left(\frac{1 - a^2 - abe^{-\beta h_b} + \sqrt{1 - a^2}\sin\gamma_b}{1 - a^2 - abe^{-\beta h} + \sqrt{1 - a^2}\sin\gamma}\right)\right] \tag{20b}$$

and, finally, for $a^2 > 1$,

$$\Gamma(\gamma,h) = \pm \frac{a}{\sqrt{a^2 - 1}}\left\{\sin^{-1}\left[\frac{\beta e^{\beta h}}{K_2}(1 - a\cos\gamma)\right] - \sin^{-1}\left[\frac{\beta e^{\beta h_b}}{K_2}\left(1 - a\cos\gamma_b\right)\right]\right\} \tag{20c}$$

In equations (20b) and (20c), the negative sign in the term on the right is proper for all cases run in positive time, and the positive sign is proper for cases run in negative time.

Numerical Examples

Using the exact equations of motion given by equations (1), a set of six trajectories were run on a digital computer. This computation was done in order to obtain exact trajectories with which the approximate equations could be compared. A summary of the trajectory characteristics is shown in table I. The breakout conditions for these cases were taken from an actual simulation which will be discussed later in the report. These trajectories were run in negative time from the final condition and thus represent the last few seconds just before skipout.

The computational procedure used in solving the approximate equations is as follows:

(1) For each of the six cases, the breakout conditions V_b, γ_b, and h_b are specified. The altitude is supplied at all times from the exact solutions; thus, the altitude becomes the independent variable for these particular test cases.

TABLE I.- CHARACTERISTICS OF THE SIX TEST TRAJECTORIES FOR FIRST ATMOSPHERIC PORTION

Trajectory	Weight, W, lb	Surface area, S, sq ft	Lift-drag ratio, L/D	For exact trajectory - Initial γ, deg	Initial V, ft/sec	Initial h, ft	Breakout flight-path angle, γ_b, deg	Breakout velocity, V_b, ft/deg	Breakout altitude, h_b, ft
I	7,000	60	0.5	5.5	35,000	300,000	2.620	24,200	300,000
II	↓	↓	↓	↓	↓	↓	2.942	24,850	↓
III							3.130	24,950	
IV							3.245	25,290	
V							3.350	25,290	
VI							3.420	25,600	

(2) Equation (9) is solved to give the corresponding approximate computed values of γ:

$$\gamma_c = \cos^{-1}\left(a + be^{-\beta h}\right)$$

(3) The values of γ from step (2) are used, along with the corresponding values of h from which they were obtained, in the solution of equation (17) for the approximate values of V.

$$V_c = V_b e^{\left[-\frac{D}{L}(\gamma_c-\gamma_b) - \frac{g}{V_b^2}(h-h_b)\right]}$$

(4) Step (2) also allows the computation of Θ. By equation (19)

$$\Theta_c = -\frac{1}{\beta r}\left[\Gamma\left(\gamma_c, \gamma_b, h, h_b\right) - \left(\gamma_c - \gamma_b\right)\right]$$

where, in the particular test cases which were studied, Θ_b is arbitrarily set at zero.

The results of numerical calculations are shown in figures 2, 3, 4, and 5. Figure 2 shows some general features of the six test trajectories. The test results for flight-path angle are presented in figure 3, the results for velocity are presented in figure 4, and the results for range are presented in figure 5. In these three figures altitude is the independent variable.

Based on the numerical calculations which are shown in figures 3, 4, and 5, the following conclusions are drawn.

First, with the possible exception of flight-path angle, the results indicate good agreement between the exact numerical solutions of the equations of motion and the approximate analytical solutions. The dependent variable in a guidance

scheme would be the lift-drag ratio of the vehicle. This ratio is, of course, governed by equation (17) in which flight-path angle may be supplied as a measured quantity if necessary.

Second, by specifying a desired set of conditions at breakout, one can obtain complete convergence of the approximate and exact solutions. As a consequence, these equations should be especially suitable for guiding a vehicle during the final critical stages of the skipout maneuver.

Guidance Implications

Thus far, it has been shown that the equations which have been developed will actually describe the motions of a

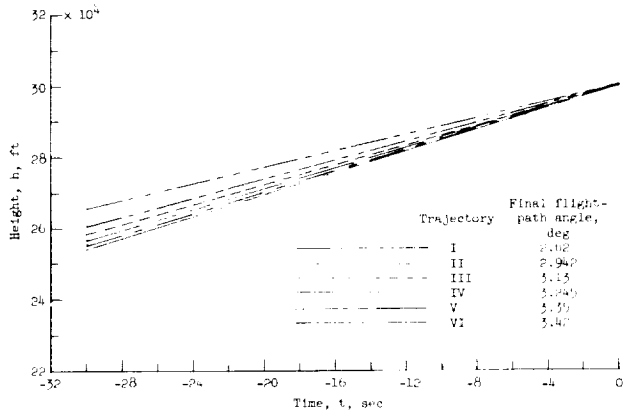

Figure 2.- Altitude plotted against time for six test trajectories during final 30 seconds before breakout.

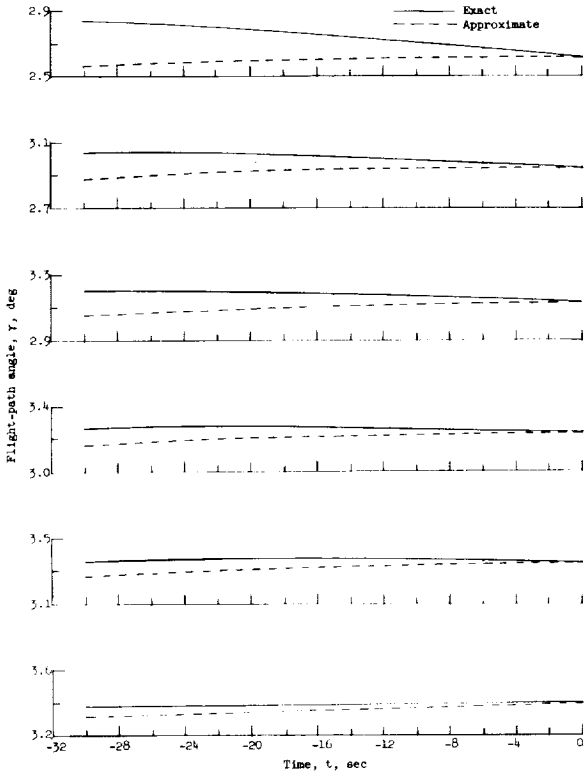

Figure 3.- Comparison of flight-path angles as obtained from exact and approximate solutions to equations of motion for final 30 seconds before breakout.

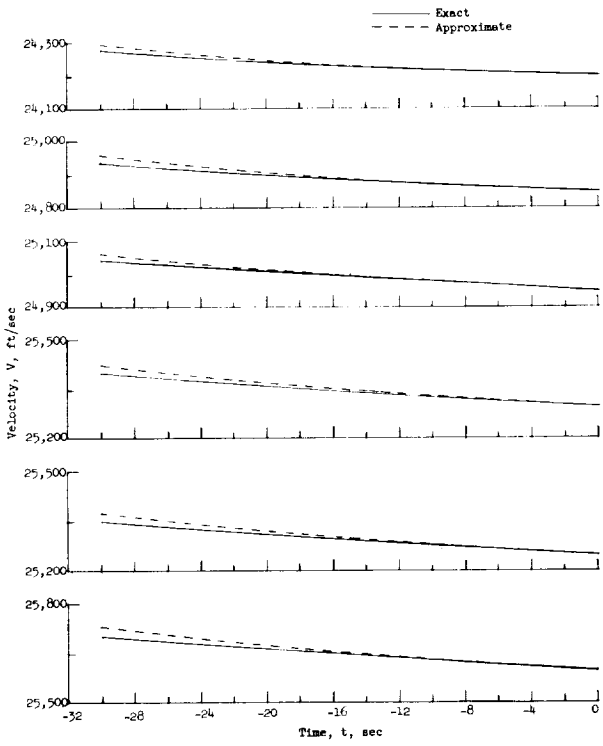

Figure 4.- Comparison of velocities as obtained from exact and approximate solutions to equations of motion for final 30 seconds before breakout.

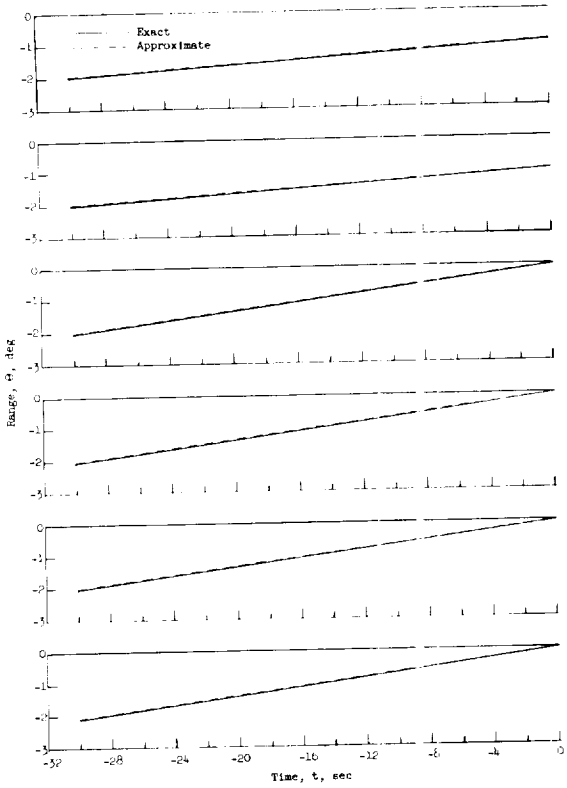

Figure 5.- Comparison of angular distance traveled about center of earth during final 30 seconds before breakout for the six test trajectories.

space vehicle within the flight regime under consideration. Given the validity of the equations, however, it is a relatively simple matter to apply them in such a manner as to control a vehicle to achieve desired exit conditions. It is to be assumed that the reentry vehicle will be equipped with an inertial guidance system or with equivalent hardware. Such a system, if alined just prior to reentry, would be able to supply information such as present altitude, velocity, and possibly flight-path angle. If information were available concerning these same parameters at breakout, the dependent variable in equation (17) is the lift-drag ratio of the vehicle. Consequently, adjustments of the real lift-drag ratio in accordance with this equation will cause convergence to the desired breakout condition. The problem which remains, then, is to determine the correct breakout conditions, a problem which is best solved from orbital or ballistic considerations before entry. It is, of course, implicit in this assumption that the range to be attempted be known in advance.

COAST PHASE

A given angular range in the coast portion of a skip maneuver can theoretically be obtained with an infinite number of combinations of exit velocity and flight-path angle. One manner of obtaining uniqueness is to specify a maximum, or apogee, altitude after the skip along with the desired angular range. In such a case, however, these variables must lie within the relatively small range of angles and velocities that can be achieved in the reentry without exceeding either the deceleration limit or the angle-of-attack limit of the vehicle. There exists a requirement, therefore, that the apogee altitude be judiciously chosen in order to insure that the unique exit conditions will fall within the range of values which can actually be realized. The problem then becomes one of computing a corresponding exit velocity and flight-path angle once a desired range and skip altitude are decided upon.

Explicit equations already exist which may be used to specify range for a given exit, flight-path angle, and velocity; explicit equations also exist which may be used to specify apogee altitude for a given exit, flight-path angle, and

velocity. However, there are no explicit solutions for the reverse of this process, namely, velocity or flight-path angle in terms of range and apogee attitude. This is due to the transcendental nature of some of the trigonometric terms involved. In using the independent variables of range and apogee altitude to control skip, therefore, one has two choices. Either an iterative solution may be employed, which is essentially the same as a graphical solution, or approximate expressions may be developed which are accurate enough to suit the need. For space vehicles, probes, and so forth in flight, the latter choice is the more attractive because the computing time may be made very short and the number of computer components required may be reduced. The following set of approximate equations is developed to fill this need.

Exact Equations for Coast Range

A starting point for developing approximate equations for exit velocity and flight-path angle as functions of apogee altitude and range are the exact equations in which velocity and flight-path angle are the independent variables. The equation for range, as derived from equation (93) on page 63 of reference 3 is:

$$\theta = 2 \tan^{-1}\left[\frac{\frac{1}{2}\sin 2\gamma_b}{\left(\frac{V_{cir}}{V_b}\right)^2 - \cos^2\gamma_b}\right] \tag{21}$$

where the subscript b denotes conditions existing at exit from the atmosphere and V_{cir} is circular satellite velocity at 300,000 feet. The equation for maximum altitude is (see appendix)

$$h_a = \frac{-B \pm \sqrt{B^2 - 4AC}}{2A} - r_e \tag{22}$$

where

$$A = V_b^2 - \frac{2g_e r_e^2}{r_b} \tag{23}$$

$$B = 2g_e r_e^2 \tag{24}$$

and

$$C = -\left(r_b V_b \cos \gamma_b\right)^2 \tag{25}$$

Values of V_b and γ_b which satisfy both equations (21) and (22) simultaneously are the values which give a particular maximum altitude for a particular range.

Approximate Equations for Coast Range

By use of the following substitution, equation (21) may be put into a form which is much easier to manipulate. Let

$$\dot{x} = V_b \cos \gamma_b \tag{26}$$

and

$$\dot{z} = V_b \sin \gamma_b \tag{27}$$

Then, beginning with equation (21),

$$\theta = 2 \tan^{-1}\left[\frac{\left(V_b \sin \gamma_b\right)\left(V_b \cos \gamma_b\right)}{V_{cir}^2 - \left(V_b \cos \gamma_b\right)^2}\right] = 2 \tan^{-1}\left(\frac{\dot{x}\dot{z}}{V_{cir}^2 - \dot{x}^2}\right) \tag{28}$$

which can be put into the form

$$\dot{x}^2 + \left(\dot{z} \operatorname{ctn} \frac{\theta}{2}\right)\dot{x} - V_{cir}^2 = 0$$

the $\dot{x}$ term of which is

$$\dot{x} = -\frac{\dot{z}}{2} \operatorname{ctn} \frac{\theta}{2} \pm \sqrt{V_{cir}^2 + \left(\frac{\dot{z}}{2} \operatorname{ctn} \frac{\theta}{2}\right)^2} \tag{29}$$

The second term under the radical sign is numerically of magnitude much smaller than V_{cir}^2, and hence may be neglected. After this second term is dropped, equation (29) becomes

$$\dot{x} = V_{cir} - \frac{\dot{z}}{2} \operatorname{ctn} \frac{\theta}{2} \tag{30}$$

Equation (30) is approximately equivalent to equation (28) under almost all conditions likely to be encountered in practice, and the approximation becomes invalid only near $\theta = 0^\circ$ and $\theta = 360^\circ$. Whereas it was not possible to solve equations (21) and (22) explicitly, it is possible to solve equations (30) and (22).

Rewriting equation (23) gives

$$A = \dot{x}^2 + \dot{z}^2 - \frac{2g_e r_e^2}{r_b} \tag{31}$$

Solving for $\dot{z}^2$ yields

$$\dot{z}^2 = A - \dot{x}^2 + \frac{2g_e r_e^2}{r_b} \tag{32}$$

But, from equation (22),

$$\left(2Ar_a + B\right)^2 = B^2 - 4AC$$

where $r_a = h_a + r_a$ is the highest or apogee radius. Now,

$$A\left(Ar_a^2 + Br_a + C\right) = 0$$

therefore,

$$A = -\frac{B}{r_a} - \frac{C}{r_a^2} \tag{33}$$

so that

$$\dot{z}^2 = -\frac{B}{r_a} - \frac{C}{r_a^2} - \dot{x}^2 + \frac{2g_e r_e^2}{r_b} \tag{34}$$

Inasmuch as equations (25) and (26) can be combined to form

$$C = -\dot{x}^2 r_b^2 \tag{35}$$

equation (35) may be substituted in equation (34) so that

$$\dot{z}^2 = -\frac{B}{r_a} + \frac{r_b^2 \dot{x}^2}{r_a^2} - \dot{x}^2 + \frac{2g_e r_e^2}{r_b}$$

$$\dot{z}^2 = -\frac{B}{r_a} + \left(\frac{r_b^2}{r_a^2} - 1\right)\dot{x}^2 + \frac{2g_e r_e^2}{r_b} \tag{36}$$

But, from equation (26),

$$\dot{x}^2 = V_{cir}^2 - V_{cir}\,\dot{z}\,\operatorname{ctn}\frac{\theta}{2} + \frac{\dot{z}^2}{4}\operatorname{ctn}^2\left(\frac{\theta}{2}\right) \tag{37}$$

Again, dropping the small last term on the right-hand side of equation (37) which is negligible in relation to V_{cir}^2, and then substituting equation (37) into equation (36) yields

$$\dot{z}^2 = -\frac{B}{r_a} + \left(\frac{r_b^2}{r_a^2} - 1\right)\left(V_{cir}^2 - V_{cir}\dot{z}\,\operatorname{ctn}\frac{\theta}{2}\right) + \frac{2g_e r_e^2}{r_b} \tag{38}$$

After collection of terms, equation (38) becomes

$$\dot{z}^2 + \left[\left(\frac{r_b^2}{r_a^2} - 1\right)V_{cir}\operatorname{ctn}\frac{\theta}{2}\right]\dot{z} + \left[\frac{B}{r_a} - \left(\frac{r_b^2}{r_a^2} - 1\right)V_{cir}^2 - \frac{2g_e r_e^2}{r_b}\right] = 0 \tag{39}$$

Defining

$$A' = 1 \tag{40}$$

$$B' = V_{cir}\left(\frac{r_b^2}{r_a^2} - 1\right)\operatorname{ctn}\frac{\theta}{2} \tag{41}$$

and

$$C' = \frac{B}{r_a} - \left(\frac{r_b^2}{r_a^2} - 1\right)V_{cir}^2 - \frac{2g_e r_e^2}{r_b} \tag{42}$$

then

$$\dot{z} = \frac{-B' \pm \sqrt{(B')^2 - 4A'C'}}{2A'} \tag{43}$$

Because a negative $\dot{z}$ will not permit skipout, the positive sign on the radical is selected.

It follows immediately once $\dot{z}$ is known that $\dot{x}$ can be calculated from equation (30). Hence, from equations (26) and (27)

$$V_b = \sqrt{\dot{x}^2 + \dot{z}^2} \tag{44}$$

and

$$\gamma_b = \cos^{-1}\left(\frac{\dot{x}}{V_b}\right) \tag{45}$$

Comparison of Approximate Solutions With Exact Solutions

Solutions to these equations were computed both for the exact equations (15) and (19) and also for the approximate equations in order to compare the results of the two methods. Figure 6 is an exact solution to equations (18) and (19) where the dashed lines are lines of constant apogee and the solid lines are lines of constant range. The corresponding approximate solutions are shown in figure 7, to the same scale, for a number of ranges and apogee altitudes.

Figure 8 shows the same information as figure 6; however, in this case, V_b and γ_b are broken up into $\dot{x}$ and $\dot{z}$. The peculiar, fan-like structure of this curve converging toward V_{cir} is of interest. In all of the cases shown here, the reference altitude is taken at 300,000 feet. For higher altitudes, the fan tends to be closed somewhat towards the 180° line. Figure 9 gives the same information for the approximate equations as does figure 8 for the exact. Figure 10 is a comparison of the approximate-range equation (26) with the exact-range equation in order to give an idea of the discrepancy between the two. It can be seen that no significant loss in accuracy results from the use of the approximate equations.

Inasmuch as atmospheric drag may be neglected above the breakout altitude of 300,000 feet for all practical purposes, the foregoing set of equations (eqs. (30), (43), (44), and (45)) may be used to predict exit conditions for the atmospheric portion of the maneuver. Moreover, due to their explicit nature, they will be able to do this more quickly than would be the case with more exact solutions.

GUIDANCE SCHEME AND SIMULATION

The two sets of approximate equations which have been developed may now be combined to form a single guidance scheme. Such a guidance scheme would be somewhat as follows.

A range to be sought is decided upon before or during the early skip phase of the maneuver. This range must, of course, lie within the set of ranges which are physically realizable.

A unique combination of breakout velocity and flight-path angle which will achieve this range is determined from the strictly orbital considerations of the coast phase. Factors which govern the selection of this combination, for instance, are the maximum or minimum allowable altitude after the first skip.

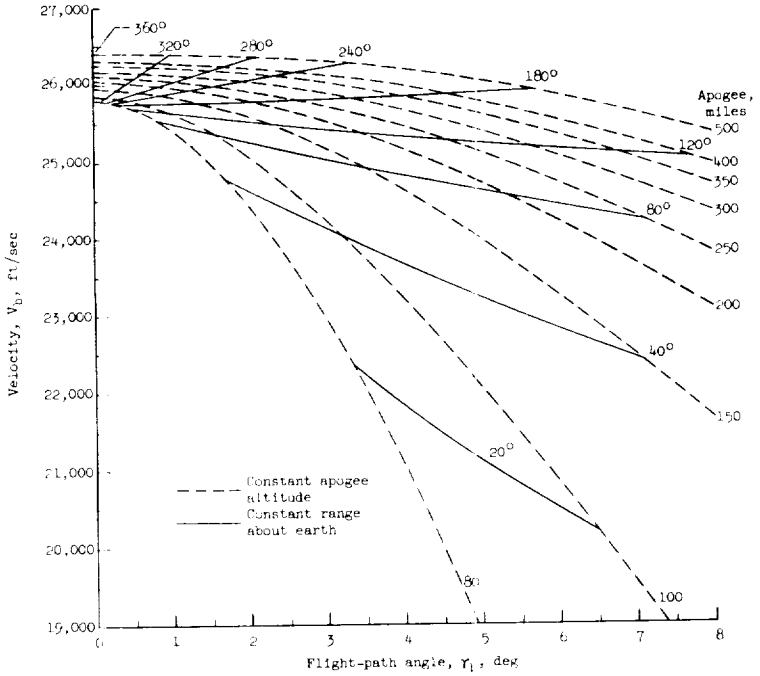

Figure 6.- Exit velocity plotted against flight-path angle showing lines of constant range and apogee altitude for exact computation.

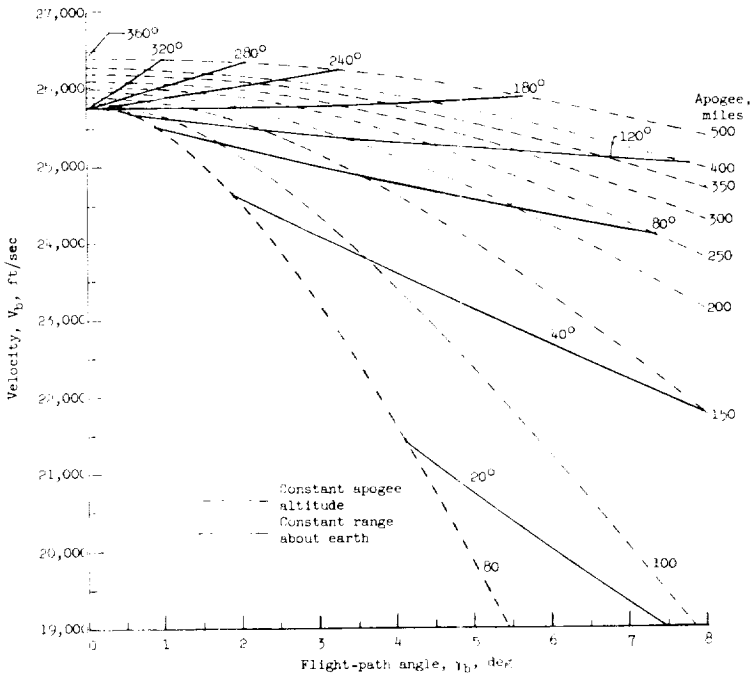

Figure 7.- Approximate solutions showing lines of constant range and apogee altitude.

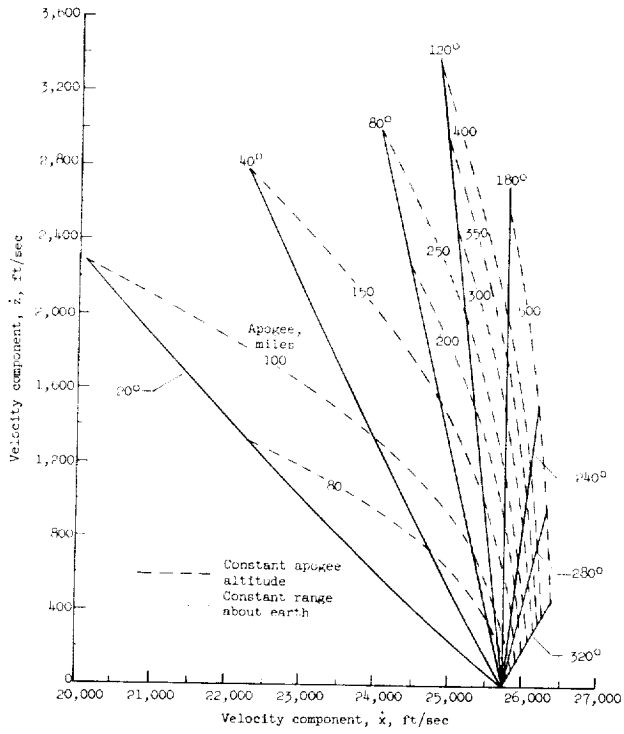

Figure 8.- Vertical and horizontal components of exit velocity showing lines of constant range and apogee.

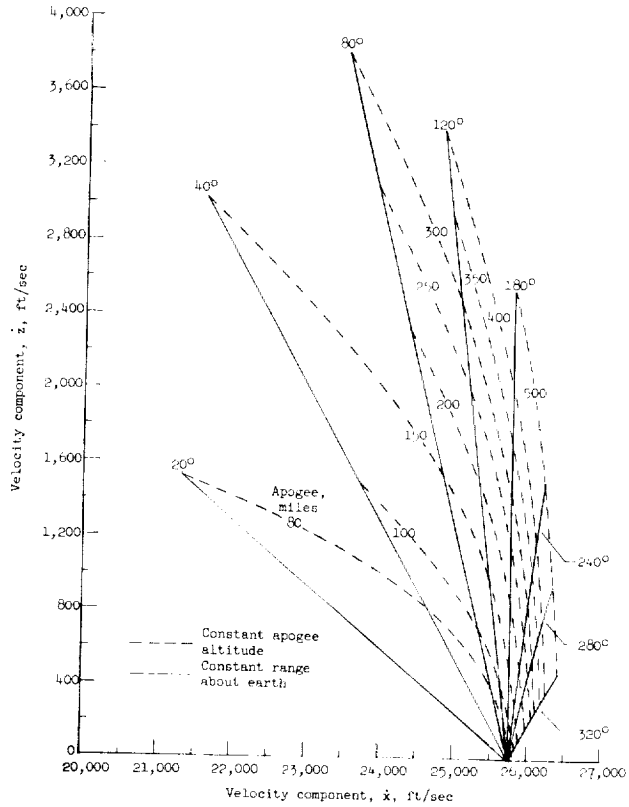

Figure 9.- Approximate solutions showing vertical and horizontal components of exit velocity with lines of constant range and apogee.

At some time during the skip, probably just as the vehicle starts to climb out, a control computer begins solving the approximate equations. This computer will receive inputs from an inertial guidance system detailing present velocity, flight-path angle, and altitude. This information is then used along with the desired final flight-path angle and velocity in equation (14) to select the proper lift-drag ratio. The procedure is repeated continuously, all terms becoming increasingly accurate until breakout is reached, at which time the desired final conditions should be achieved. The vehicle then follows the usual Keplerian orbit until the second reentry.

The skip-control scheme which is outlined here was programed on a digital computer in order to check its validity. Some of the preliminary results of this simulation scheme are listed in table II. A block diagram of the simulation is given in figure 11. The results shown in the table are for a vehicle which has the lift-drag characteristics of figure 12, and which weighs 7,000 pounds and has a surface area of 60 square feet. A limit to the angle of attack corresponding to a lift-drag ratio of 0.5 was incorporated. Entry was at 35,000 feet per second with initial flight-path angles of -5°, -5.5°, and -6° at 300,000 feet, although other entry conditions have been studied. The atmosphere used in this simulation is the ARDC Model Atmosphere, 1959 (ref. 4). The proper apogee altitude after

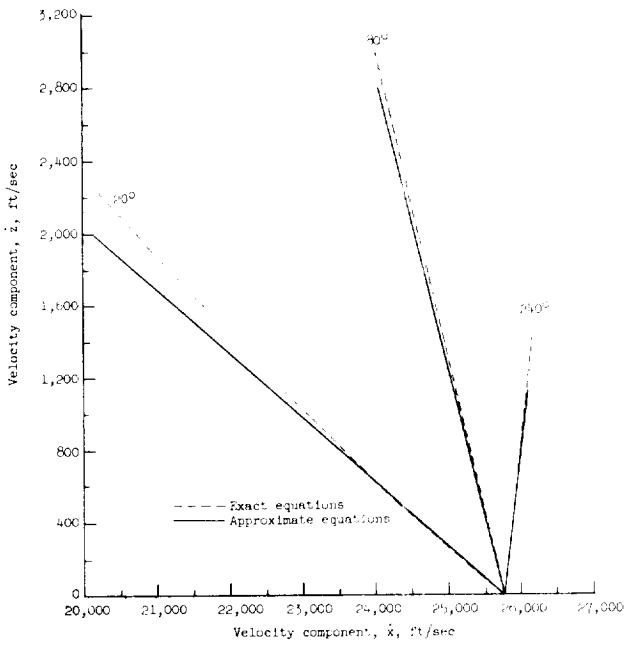

Figure 10.- Comparison of range obtained by approximate and exact equations.

the skip for each desired range was selected empirically because a good analytic selection technique is not presently available. Under present circumstances, this would have to be read into the guidance from tables. Interpolation here is practical since great accuracy is not required. The results indicate agreement between the desired and achieved exit velocities to within approximately 4 feet per second, and, in most cases where the desired velocity has been achieved, the desired flight-path angle has also been achieved to within one-tenth of a degree. Selected time histories from this simulation are shown in figures 13, 14, and 15. In this simulation, guidance was initiated at minimum altitude and continued until breakout. Thus, the guidance mode was in operation during roughly the final 60 seconds before breakout. Ranges between roughly 70° and 200° about the center of the earth are easily achieved

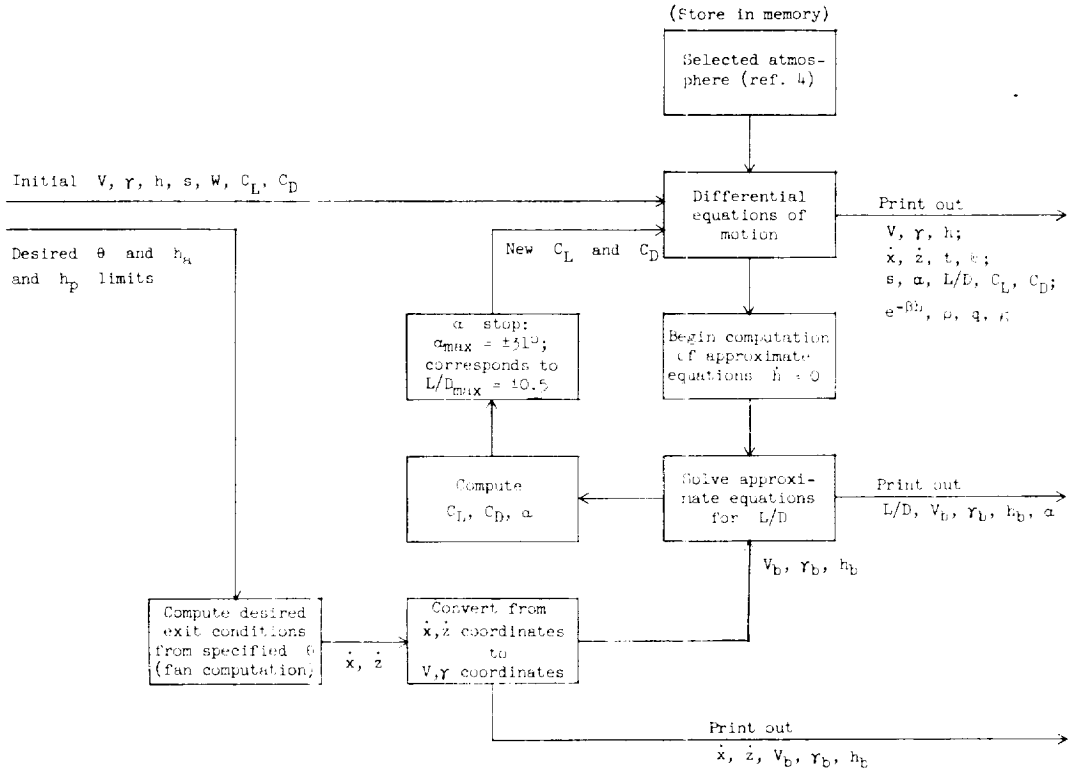

Figure 11.- Block diagram of simulation.

TABLE II.- TYPICAL SIMULATION RESULTS

Entry angle, deg	Desired range, θ, deg	Apogee, h_a, ft	Desired exit velocity, V_b, ft/sec	Exit velocity, V_b, ft/sec	Desired exit flight-path angle, γ_b, deg	Exit flight-path angle, γ_b, deg
-5	101.50	656,000	25,407	25,407	1.96	1.92
	132.82	820,000	25,564	25,568	2.05	2.04
	158.52	984,000	25,676	25,676	2.11	2.11
	179.68	1,148,000	25,764	25,768	2.16	2.16
	197.22	1,312,000	25,843	25,843	2.20	2.21
-5.5	45.02	492,000	24,423	24,426	2.63	2.31
	71.48	656,000	24,892	24,895	2.94	2.80
	94.41	820,000	25,151	25,151	3.12	3.04
	114.48	984,000	25,328	25,328	3.25	3.21
	132.14	1,148,000	25,463	25,463	3.35	3.32
	147.70	1,312,000	25,571	25,574	3.43	3.42
-6	33.32	492,000	23,304	23,304	3.67	2.97
	53.94	656,000	24,138	24,141	4.04	3.69
	72.70	820,000	24,584	24,587	4.22	4.01
	90.00	984,000	24,879	24,879	4.34	4.19
	105.90	1,148,000	25,092	25,095	4.41	4.32
	120.52	1,312,000	25,263	25,263	4.47	4.40

with a slight loss in accuracy in flight-path angle when shorter ranges are attempted. Actually this loss of accuracy does not represent any significant loss in range capability inasmuch as the sensitivity of range to flight-path angle is also less in this region. Longer ranges were not attempted because the higher apogee altitudes involved were not deemed desirable.

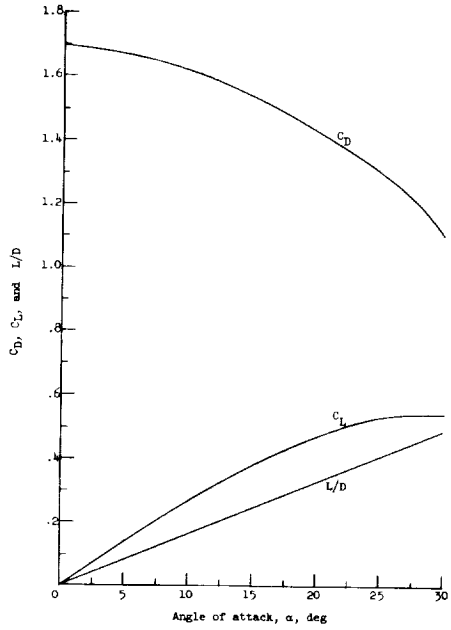

Figure 12.- Aerodynamic characteristics of vehicle.

CONCLUSIONS

As a result of the foregoing studies of the initial reentry and coast portions of a skip maneuver, the following general conclusions may be drawn:

1. The approximate guidance equations for the atmospheric portion of the skip show promise of providing suitable guidance for a vehicle during the critical final 60 seconds or so before breakout from the atmosphere to some

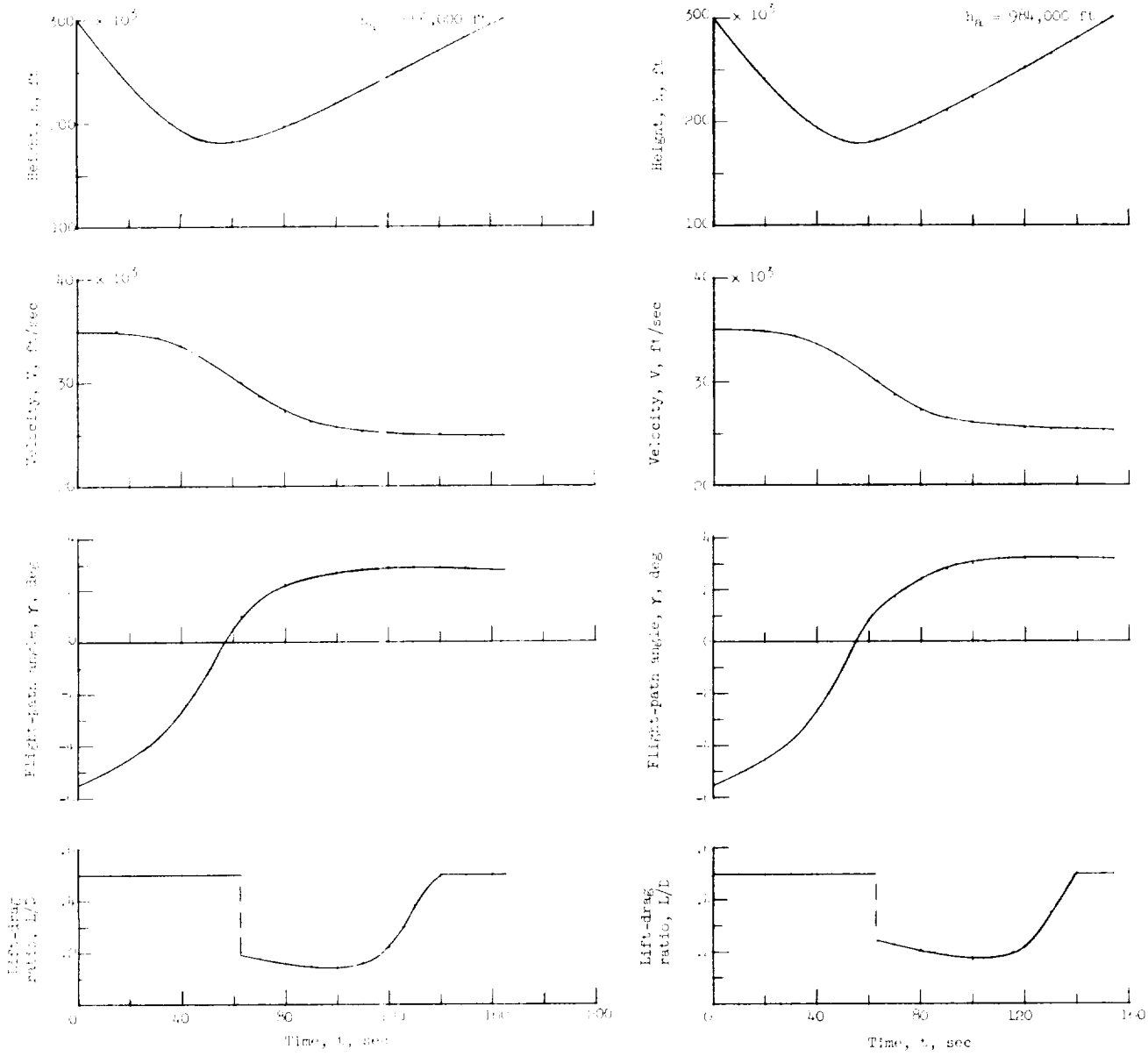

(a) Minimum range: 71.48°. (b) Intermediate range: 114.48°.

Figure 13.- Time histories of simulation studies for minimum, intermediate, and maximum ranges, all with entry flight-path angle of $-5\frac{1}{2}^{\circ}$.

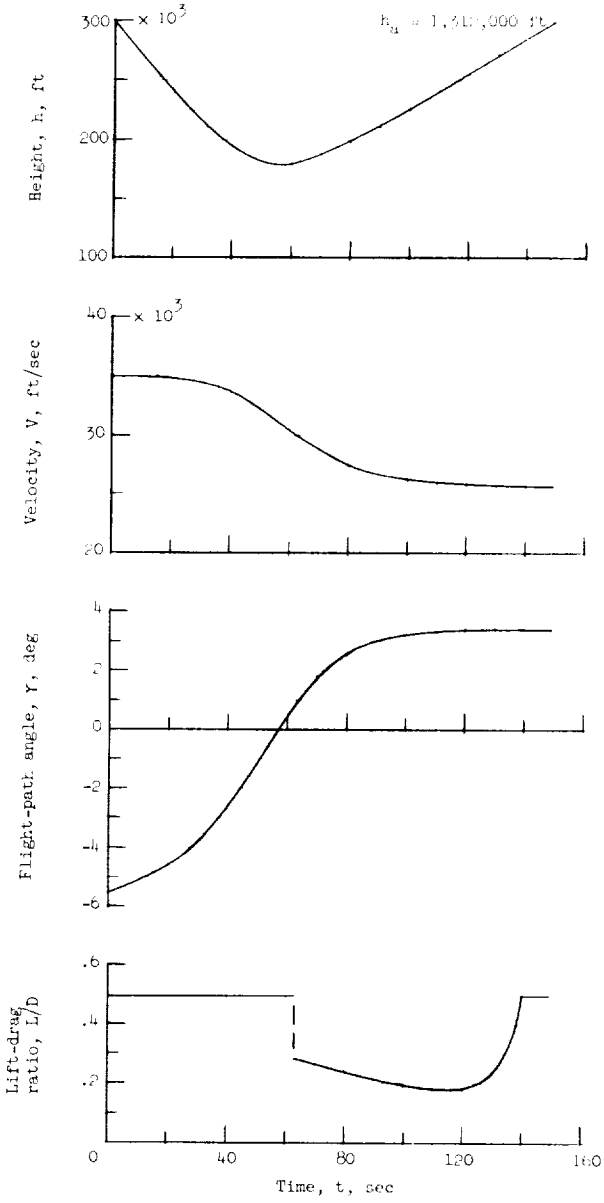

(c) Maximum range: 147.70°.

Figure 13.- Concluded.

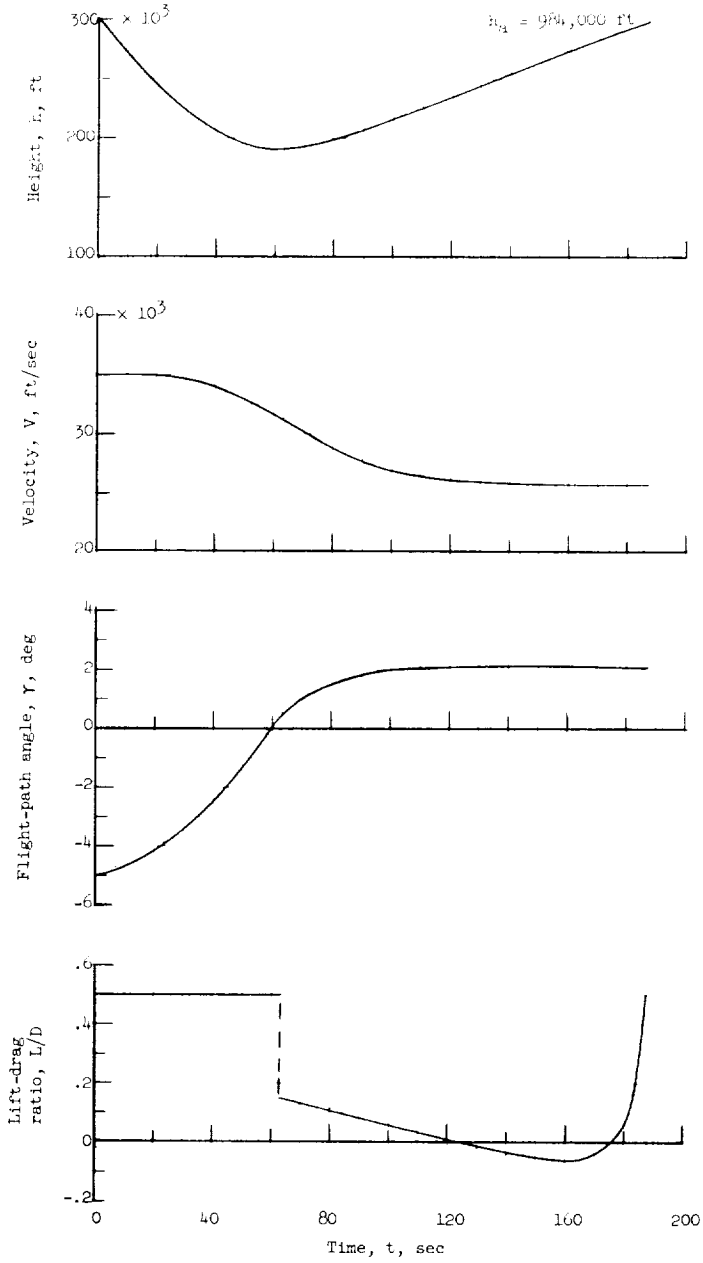

Figure 14.- Time history of simulation study with entry flight-path angle of -5° and intermediate range of 158.52°.

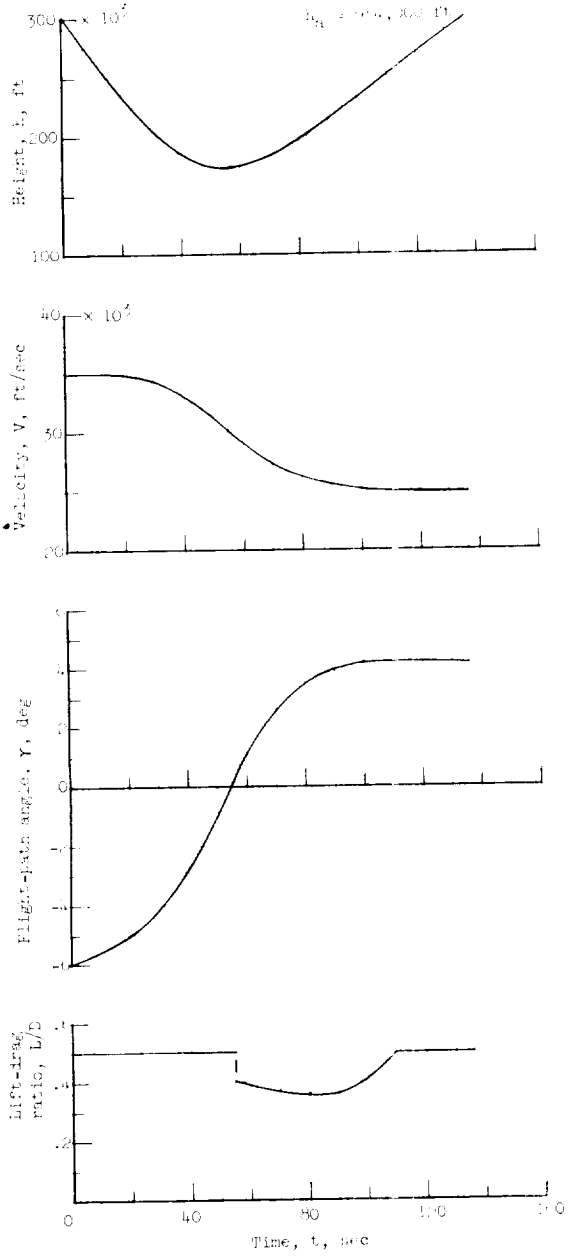

Figure 15.- Time history of simulation study with entry flight-path angle of -6° and intermediate range of 90.00°.

previously specified breakout velocity and flight-path angle. The principal reason for this fact is attributed to the convergent nature of the equations as the vehicle approaches breakout altitude which insures that breakout conditions will be achieved precisely and accurately.

2. The equations governing the atmospheric portion display the desirable property of simplicity and, hence, require a minimum of computer storage space. As a result, they may be stored in a separate memory core and need not be read into the guidance computer at all unless actually needed.

3. As a result of the explicit nature of these equations, they may be solved rapidly on a digital computer and may thus be used to govern the control inputs of the vehicle based on vehicle conditions at the time of computation.

4. Exit conditions in terms of velocity and flight-path angle may be specified uniquely by a desired range and some corresponding maximum altitude after the skipout. When the exit conditions are taken to exist at some specified reference altitude above the discernible atmosphere, these exit conditions are suitable for specifying the breakout conditions for the atmospheric portion of the skip.

5. No significant loss in accuracy occurs when the approximate equations are used in preference to the exact equations for specifying breakout conditions in terms of range and apogee altitude, whereas, by this means, a simplification may be achieved in the computational procedure which results in a corresponding reduction in the computer requirements.

6. The preliminary results of a digital-computer simulation of the guidance scheme suggested in this paper

indicate that it does work for a variety of desired ranges, achieving the desired exit velocity within 4 feet per second and the desired exit flight-path angle within one-tenth of a degree of those values which are specified for the coast phase. Entries at 35,000 feet per second with flight-path angles between -5° and -6° at 300,000 feet may be guided with good accuracy to ranges between 70° and 200° about the center of the earth.

Langley Research Center,
National Aeronautics and Space Administration,
Langley Station, Hampton, Va., April 24, 1963.

APPENDIX

DERIVATION OF THE EQUATION FOR MAXIMUM ALTITUDE

The equation for maximum altitude (eq. (19) of text) may be obtained from the conservation of momentum and energy. The following equation is given for the conservation of momentum:

$$r_b V_b \cos \gamma_b = r_a V_a \tag{A1}$$

where the subscript a refers to apogee conditions. Inasmuch as $r_a = h_a + r_e$, solving for V_a^2 yields

$$V_a^2 = \left(\frac{r_b V_b \cos \gamma_b}{r_e + h_a} \right)^2 \tag{A2}$$

From the equation for the conservation of energy,

$$V_a^2 - \frac{2 g_e r_e^2}{r_a} = V_b^2 - \frac{2 g_e r_e^2}{r_b} \tag{A3}$$

or, transposing and substituting for r_a,

$$V_a^2 = V_b^2 - \frac{2 g_e r_e^2}{r_b} + \frac{2 g_e r_e^2}{r_e + h_a} \tag{A4}$$

Equating equation (A4) to equation (A2) yields

$$V_b^2 - \frac{2 g_e r_e^2}{r_b} + \frac{2 g_e r_e^2}{r_e + h_a} = \frac{\left(r_b V_b \cos \gamma_b \right)^2}{\left(r_e + h_a \right)^2}$$

or

$$\left(V_b^2 - \frac{2 g_e r_e^2}{r_b} \right) \left(r_e + h_a \right)^2 + 2 g_e r_e^2 \left(r_e + h_a \right) - \left(r_b V_b \cos \gamma_b \right)^2 = 0 \tag{A5}$$

If the following substitutions are made (eqs. (23), (24), and (25), respectively, of the text):

$$A = V_b^2 - \frac{2 g_e r_e^2}{r_b}$$

$$B = 2g_e r_e^2$$

$$C = -\left(r_b V_b \cos \gamma_b\right)^2$$

then

$$h_a = \frac{-B \pm \sqrt{B^2 - 4AC}}{2A} - r_e$$

It is clear that only the positive root will give physically meaningful results.

REFERENCES

1. Eggleston, John M., and Young, John W.: Trajectory Control for Vehicles Entering the Earth's Atmosphere at Small Flight-Path Angles. NASA TR R-89, 1961. (Supersedes NASA MEMO 1-19-59L.)

2. Wang, Kenneth, and Ting, Lu: Approximate Solutions for Reentry Trajectories With Aerodynamic Forces. PIBAL Rep. No. 647 (Contract No. AF 49(638)-445), Polytechnic Inst. Brooklyn, May 1961.

3. Berman, Arthur I.: The Physical Principles of Astronautics. John Wiley & Sons, Inc., c.1961.

4. Minzner, R. A., Champion, K. S. W., and Pond, H. L.: The ARDC Model Atmosphere, 1959. Air Force Surveys in Geophysics No. 115 (AFCRC-TR-59-267), Air Force Cambridge Res. Center, Aug. 1959.

NASA-Langley, 1963 L-3210